International Journal of Modern Physics B
Vol. 31 (2017) 1750250 (16 pages)

DOI: 10.1142/S0217979217502502

Ultrasonic wave generation in two-band organic conductors due to thermoelectric effect

Danica Krstovska

Faculty of Natural Sciences and Mathematics,
Ss. Cyril and Methodius University,
Arhimedova 5, 1000 Skopje, Macedonia
danica@pmf.ukim.mk
krstovska@magnet.fsu.edu

Received 23 March 2017
Revised 15 May 2017
Accepted 8 June 2017
Published 26 July 2017

A linear thermoelectric generation of a longitudinal ultrasonic wave in organic conductors with two conducting channels, quasi-one dimensional (q1D) and quasi-two dimensional (q2D), is investigated theoretically. The magnetic field and temperature dependences of the amplitude of generated through Nernst effect wave in $\alpha-(\mathrm{BEDT}-\mathrm{TTF})_2\mathrm{KHg(SCN)}_4$ for two boundary conditions, isothermal and adiabatic are obtained. Findings show a preference of one type of a boundary over another in the wave generation and propagation depending on the magnetic field strength and temperature. At lower temperatures and above $B = 4$ T, the wave amplitude for adiabatic boundary is smaller compared to the one for isothermal boundary although there is a heat flux through the conductor's surface in the latter. Both the q1D and q2D charge carriers contribute to the observation of the effect but with different magnitude due to the different drift velocity along the direction of wave propagation.

Keywords: Two-band organic conductors; ultrasonic waves generation; Nernst effect.

PACS numbers: 43.20.+g, 72.15.Eb, 72.15.Jf

1. Introduction

In recent decades the interest in investigations of electron phenomena in multilayered structures of organic origin rose considerably because of their great importance for applied sciences. For understanding electron processes in such structures information about the energy spectrum of the charge carriers is necessary. A considerable group of layered organic conductors has multi-sheeted Fermi surface (FS),

and therefore consists of various topological elements such as a weakly corrugated quasi-two-dimensional (q2D) cylinder of holes and a pair of quasi-one-dimensional (q1D) electron sheets, for example, the FS of organic conductors based on tetrathiafulvalene $\kappa - (\mathrm{BEDT-TTF})_2\mathrm{Cu(SCN)}_2$ and $\alpha - (\mathrm{BEDT-TTF})_2\mathrm{MHg(SCN)}_4$ where M is one of the metals K, Rb, Tl or NH_4. The energy spectrum of these conductors is quite complicated as two charge carrier groups with q1D and q2D energy spectra are responsible for the charge transport.[1,2] These crystalline organic metals, being very clean and having extremely large anisotropy of electronic properties, have attracted much attention as excellent objects for studying specific features of certain phenomena including the thermoelectric generation of ultrasonic waves by using noncontact ultrasonic techniques.

Electromagnetic, thermal and acoustic waves form a coupled system that permits their mutual transformation.[3,4] When an electromagnetic wave of frequency ω is incident on the surface of the conductor, nonuniform temperature oscillations of the same frequency ω appear due to the thermoelectric force.[5] The temperature oscillations generate thermoelectric stresses which in turn induce in the conductor acoustic oscillations with the same frequency.[6] This phenomenon is known as a thermoelectric generation of acoustic waves. It is manifested only under the conditions of normal skin effect, when the electron mean-free path length l is much smaller than the penetration depth of both the electromagnetic δ_E and thermal field δ_T in the conductor, $l \ll \delta_E, \delta_T$.

Thermoelectric generation of ultrasonic waves is of interest for studying the acoustic properties of conductors as well as for determining the coupling parameters between the electronic, ionic and spin subsystems.

In isotropic metals, the thermoelectric generation of acoustic waves has been studied in number of papers[5,7–11] but in organic conductors it has been considered in those with only one conducting channel, i.e., in organic conductors with q2D group of charge carriers.[12] Their FS is by far simpler than the FS of two-band organic conductors and consists of a corrugated cylinder open in the direction of the normal with respect to the layers.

In this work, the generation of ultrasonic waves due to Nernst effect for both isothermal and adiabatic boundary thermal conditions is studied. To clarify the specific features of the generation and propagation of ultrasonic waves in low-dimensional conductors excited by the Nernst effect, two-band layered organic conductors (with two conducting channels, q1D and q2D), are considered. The role played by the constant, relatively high, but nonquantizing magnetic field in the linear thermoelastic generation of ultrasonic waves has been investigated. The purpose of this study is to explore the changes in the amplitude of the generated ultrasonic wave with the magnetic field and its orientation in multi-layered systems through how the thermoelectric properties change with the magnetic field's magnitude and direction. This work uses and complements the study of magnetic-field and angle-dependent Nernst effect in two-band organic conductors arising from the q1D and q2D FS.

2. Theoretical Model for Linear Thermoelectric Generation of Ultrasonic Waves

In a conducting medium, the temperature oscillations induce only longitudinal acoustic oscillations. Suppose that an electromagnetic wave ($E_x = E_z = 0, E_y = E$) of frequency ω is incident normally on a surface along the less conductivity axis (z-axis) i.e., $\mathbf{k} = (0, 0, k)$ of a two-band organic conductor. The magnetic field is applied along an arbitrary angle, i.e., $\mathbf{B} = (B\cos\phi\sin\theta, B\sin\phi\sin\theta, B\cos\theta)$ and its orientation is varied from the z-axis to the conducting plane, xy-plane. θ represents the angle between the z-axis and xy-plane and ϕ represents the angle from the x-axis in the xy-plane.

In order to calculate the amplitude of the generated by Nernst effect longitudinal ultrasonic wave, the temperature distribution associated with the oscillations of the electromagnetic field must be determined first. The temperature distribution within the conductor can be obtained by using the thermal conduction equation

$$C\frac{\partial\Theta}{\partial t} + \mathrm{div}\mathbf{q} = 0, \tag{1}$$

where Θ is the high-frequency addition to the equilibrium temperature T, C is the volumetric heat capacity and $\mathbf{q}$ is the heat flux.

The equation for the heat flux $\mathbf{q}$, which takes into account the thermoelectric effects, has the form

$$\mathbf{q} = k_B T\alpha\mathbf{j} - \kappa\nabla\Theta + Nk_B T[\mathbf{Bj}] + L[\mathbf{B}\nabla\Theta]. \tag{2}$$

Here k_B is the Boltzmann constant, α is the thermoelectric power coefficient, $\mathbf{j}$ is the current density, κ is the thermal conductivity coefficient, N is the Nernst coefficient, L is the Righi–Leduc coefficient.

The temperature oscillations lead to thermoelectric stresses σ_{ik}^{T} in the conductor

$$\sigma_{ik}^{\mathrm{T}} = -\varrho s^2\beta\Theta(z,t)\delta_{ik}, \tag{3}$$

where ρ is the density of the crystal, s is the acoustic wave velocity and β is the volumetric thermal expansion coefficient and δ_{ik} is the Kronecker delta.

These stresses induce longitudinal acoustic oscillations which amplitude is determined by means of the equation of the theory of elasticity for ionic displacement $\mathbf{U} = (0, 0, U)$

$$\varrho\frac{\partial^2 U_i}{\partial t^2} - \lambda_{iklm}\frac{\partial U_{lm}}{\partial x_k} = -\varrho s^2\beta\delta_{ik}\frac{\partial\Theta}{\partial x_k}. \tag{4}$$

Here, $U_{lm} = (1/2)(\partial U_l/\partial x_m + \partial U_m/\partial x_l)$ is the deformation tensor and λ_{iklm} are components of the elastic tensor of the crystal. The subscripts in U and x describe the wave polarization and direction of wave propagation, respectively.

As the electric field of the incident electromagnetic wave is along the y-axis the only nonzero component of the current density is the y-component, $\mathbf{j} = (0, j, 0)$. The frequency of the electromagnetic field is constraint with the condition $\omega\tau \ll 1$ where τ is the relaxation time of the conduction electrons.

Since div$\mathbf{j} = 0$, and $\nabla\Theta$ is along the z-axis (when the electromagnetic wave incidents normally on the surface of the conductor all of the quantities depend only on z) then by substituting Eq. (2) in Eq. (1) the following differential equation for the temperature distribution Θ in the conductor is obtained

$$C\frac{\partial\Theta}{\partial t} - \kappa_{zz}\frac{\partial^2\Theta}{\partial z^2} = -Nk_BT\frac{\partial}{\partial z}[\mathbf{Bj}]_z, \tag{5}$$

where κ_{zz} is the inter-layer thermal conductivity. The wave is taken to be monochromatic, so the differentiation with respect to the time variable is equivalent to multiplication by $(-i\omega)$. The current density, obtained from Maxwell's equations, has the form

$$j_y = -\frac{ik^2}{\omega\mu_0}e^{i(kz-\omega t)}, \tag{6}$$

where μ_0 is the magnetic permeability of the vacuum and

$$k = \frac{1+i}{\delta_E}, \quad \delta_E = \sqrt{\frac{2\rho_{yy}}{\omega\mu_0}}. \tag{7}$$

k and δ_E are the electromagnetic field wavenumber and penetration depth. ρ_{yy} is the in-plane component of the electric resistivity tensor ρ_{ij}. Consequently, Eq. (5) is rewritten in the following form

$$\frac{\partial^2\Theta}{\partial z^2} + k_T^2\Theta = -\frac{k_BTN_{zy}k^3B\cos\phi\sin\theta}{\omega\mu_0\kappa_{zz}}e^{ikz}, \tag{8}$$

where

$$k_T = \frac{1+i}{\delta_T}, \quad \delta_T = \sqrt{\frac{2\kappa_{zz}}{\omega C}}. \tag{9}$$

k_T and δ_T are the thermal field wavenumber and penetration depth, respectively. Equation (8) should be supplemented with the boundary conditions that describe the heat flow from the conductor. The isothermal and adiabatic boundary conditions for the temperature are

$$\Theta|_{z=0} = 0, \quad \text{and} \quad \frac{\partial\Theta}{\partial z}|_{z=0} = 0. \tag{10}$$

The amplitude of the generated longitudinal wave in the conductor is calculated from the equation of the theory of elasticity [(Eq. (4)] with $s = (\lambda_{zzzz}/\rho)^{1/2}$

$$\frac{\partial^2U_{zl}}{\partial z^2} + q^2U_{zl} = \beta\frac{d\Theta}{dz}, \tag{11}$$

where $q = \omega/s$ is the wave vector of the ultrasonic wave at frequency ω. The corresponding boundary conditions are

$$\frac{\partial U_{zl}}{\partial z}|_{z=0} = 0, \quad \text{and} \quad \frac{\partial U_{zl}}{\partial z}|_{z=0} + \beta\Theta|_{z=0} = 0. \tag{12}$$

3. Generation of a Longitudinal Ultrasonic Wave: Calculation of the Amplitude U_{zl}

The solution of Eq. (8), satisfying the boundary conditions (10), is given by

$$\Theta(z) = -\frac{k_B T N_{zy} k^3 B \cos\phi \sin\theta}{\omega \mu_0 \kappa_{zz}} \frac{1}{k_T^2 - k^2} (e^{ikz} - a e^{ik_T z}), \tag{13}$$

where $a = 1$ for the isothermal and $a = k/k_T$ for the adiabatic boundary condition. It follows from Eq. (13) that for the adiabatic boundary the temperature distribution at the conductor's surface is nonzero

$$\Theta_{|z=0} = -\frac{k_B T N_{zy} k^3 B \cos\phi \sin\theta}{\omega \mu_0 \kappa_{zz}} \frac{1}{k_T (k_T + k)}. \tag{14}$$

Assuming both groups of charge carriers have the same mean-free path length l, the effectiveness of the wave generation by Nernst effect is maximum when $q\delta_E, q\delta_T \ll 1$ until the conditions $kl \ll 1$ and $k_T l \ll 1$ are satisfied and for not very strong corrugation of the FS belonging to both the q1D and q2D charge carriers. In that case, substituting Eq. (13) in Eq. (11), and using the boundary conditions (12), the following expressions for the complex amplitude of the ultrasonic wave U_{zl}, for both isothermal and adiabatic boundary, are obtained

$$U_{zl}^i = \frac{i}{1+i} \frac{k_B T N_{zy} \beta k B \cos\phi \sin\theta}{\omega \mu_0 \kappa_{zz}} \frac{\delta_T^2}{\delta_T + \delta_E}, \tag{15}$$

$$U_{zl}^a = -2i \frac{k_B T N_{zy} \beta k B \cos\phi \sin\theta}{\omega \mu_0 \kappa_{zz} q} \frac{\delta_T^2}{\delta_E (\delta_T + \delta_E)}. \tag{16}$$

The amplitude of the generated wave is a function of the frequency of the incident electromagnetic wave ω, magnetic field B, the angle between the normal to the layers plane and the magnetic field θ, the in-plane angle ϕ as well as the characteristics of the conductor (resistivity, Nernst coefficient and thermal conductivity). The transport coefficients ρ_{yy}, N_{zy} and κ_{zz} will be calculated for the simplest model of a conductor with two groups of charge carriers. We assume that the FS consists of a pair of q1D corrugated sheets in the $p_y p_z$ plane and a corrugated cylinder extending along p_z. Represent the corresponding dispersion law of the q1D and q2D charge carriers, $\varepsilon_1(\mathbf{p})$ and $\varepsilon_2(\mathbf{p})$, in the form

$$\varepsilon_1(\mathbf{p}) = v_F(|p_x| - p_F) - 2t_b \cos\left(\frac{b p_y}{\hbar}\right) - 2t_{c1} \cos\left(\frac{c p_z}{\hbar}\right), \tag{17}$$

$$\varepsilon_2(\mathbf{p}) = \frac{p_x^2 + p_y^2}{2m^*} - 2t_{c2} \cos\left(\frac{c p_z}{\hbar}\right). \tag{18}$$

Here, x- and z-axes are associated with the most and the least conducting directions, respectively. The dispersion along the x-axis is often approximated to be linear near the Fermi level [the first term in Eq. (17)] so that v_F and p_F are the Fermi velocity and momentum of electrons belonging to the q1D sheet of the FS at $t_b = t_{c1} = 0$. b and c are the corresponding lattice constants, t_b, t_{c1} and t_{c2} are the transfer integrals, $\hbar$ is Planck's constant and m^* is the charge carrier effective mass.

For the transport coefficients to be calculated, the components of both the electrical conductivity tensor σ_{ij} and thermoelectric coefficients tensor α_{ij} must be determined first. These coefficients connect the current density $\mathbf{j}$ with the electric field $\mathbf{E}$ and temperature gradient ∇T. In order to find the relation among the current density, the electric field and the temperature gradient,

$$j_i = \frac{e}{2\pi\hbar^3}\int v_i f(\mathbf{p}) d^3p = \sigma_{ij}E_j + \alpha_{ij}\frac{\partial T}{\partial x_j}, \tag{19}$$

where e is the charge of the conduction electrons, Boltzmann transport equation for the charge carrier distribution function $f(\mathbf{p})$, based on the tight binding approximation band structure within the single relaxation time approximation τ, must be solved.[13] In Eq. (19), one must integrate over all electron states and account of the contributions into the conductivity made by each of the charge carrier groups $\sigma_{ij} = \sigma_{ij}^{(1)} + \sigma_{ij}^{(2)}$, where $\sigma_{ij}^{(1)}$ is the contribution in the conductivity from charge carriers whose states belong to the plane sheet of the FS and $\sigma_{ij}^{(2)}$ takes into account the contribution into σ_{ij} made by the rest of the carriers.

In the presence of a weak electric field and temperature gradient along the z-axis of the conductor the transport equation assumes the following form

$$\frac{\partial\Psi}{\partial t_B} + \frac{\Psi}{\tau} = e\mathbf{E}\mathbf{v} + \frac{\varepsilon-\mu}{k_BT}\mathbf{v}\nabla T, \tag{20}$$

where $\Psi\frac{\partial f_0}{\partial\varepsilon}$ is the nonequilibrium correction to the equilibrium electron distribution function $f_0(\varepsilon)$, μ is the chemical potential of the electron system and t_B is the time of motion of the conduction electrons in a magnetic field with a period $T_p = 2\pi/\omega_c$ and cyclotron frequency $\omega_c = eB\cos\theta/m^*$.

The solution of Eq. (20) is written in the following form

$$\Psi_i = eE_i\int_{-\infty}^{t} dt' v_i(t') e^{\frac{t'-t}{\tau}} - \frac{\partial T}{\partial x_i}\int_{-\infty}^{t} dt' \frac{\varepsilon-\mu}{k_BT} v_i(t') e^{\frac{t'-t}{\tau}} \tag{21}$$

and makes it possible to determine the electrical conductivity tensor components

$$\sigma_{ij} = \frac{2e^3B}{(2\pi\hbar)^3}\int\frac{\partial f_0}{\partial\varepsilon}d\varepsilon\int dp_B\int_0^{T_p} dt v_i(t)\Psi_j \tag{22}$$

as well as the thermoelectric tensor components

$$\alpha_{ij} = \frac{2e^2B}{(2\pi\hbar)^3}\int\frac{\varepsilon-\mu}{k_BT}\frac{\partial f_0}{\partial\varepsilon}d\varepsilon\int dp_B\int_0^{T_p} dt v_i(t)\Psi_j. \tag{23}$$

Here, $p_B = p_x\sin\theta\cos\phi + p_y\sin\theta\sin\phi + p_z\cos\theta = \text{const}$ is the momentum component along the magnetic field $\mathbf{B}$.

The motion of the conduction electrons in a magnetic field is described by the following equations of motion

$$\frac{\partial p_x}{\partial t} = e\mu_0 B\cos\theta(v_y - v_z\sin\phi\tan\theta), \tag{24}$$

$$\frac{\partial p_y}{\partial t} = e\mu_0 B\cos\theta(v_z\cos\phi\tan\theta - v_x), \tag{25}$$

$$\frac{\partial p_z}{\partial t} = e\mu_0 B \sin\theta (v_x \sin\phi - v_y \cos\phi). \tag{26}$$

The electrical conductivity σ_{zz} and thermoelectric coefficient α_{zz} across the layers

$$\sigma_{zz} = -\frac{2e^2}{(2\pi\hbar)^3} \int \frac{\partial f_0}{\partial \varepsilon} d\varepsilon \int_0^{\frac{2\pi\hbar\cos\theta}{c}} dp_B 2\pi m^* \bar{v}_z^2 \tau, \tag{27}$$

$$\alpha_{zz} = \frac{2e}{(2\pi\hbar)^3} \int \frac{\varepsilon - \mu}{k_B T} \frac{\partial f_0}{\partial \varepsilon} d\varepsilon \int_0^{\frac{2\pi\hbar\cos\theta}{c}} dp_B 2\pi m^* \bar{v}_z^2 \tau, \tag{28}$$

depend substantially on the average inter-layer electron velocity $\bar{v}_z$ on an electron orbit $\varepsilon = \text{const}$ and $p_B = \text{const}$.

In τ-approximation, it is sufficient to calculate the components of the electrical conductivity tensor and the rest of the kinetic coefficients, describing the heat flux and thermoelectric effects, are obtained from the following relations:

$$\alpha_{zz} = \frac{\pi^2 k_B T}{3e} \frac{\partial \sigma_{zz}}{\partial \varepsilon}\bigg|_{\varepsilon=\mu}, \tag{29}$$

$$\kappa_{zz} = \frac{\pi^2 k_B^2 T}{3e^2} \sigma_{zz}, \tag{30}$$

$$N_{zy} = \frac{\alpha_{zz}}{\sigma_{zy}}. \tag{31}$$

After averaging Eq. (24) over a sufficiently long time interval about the order of the mean free time of electron, one obtains the following relation for the in-plane electron velocity v_y from both the q1D and q2D charge carriers

$$\bar{v}_y^{\text{q1D, q2D}} = \bar{v}_z^{\text{q1D, q2D}} \sin\phi \tan\theta. \tag{32}$$

The inter-layer velocity of the q1D and q2D charge carriers is calculated by using the corresponding energy dispersion law [Eqs. (17) and (18)]

$$\begin{aligned} \bar{v}_z^{\text{q1D, q2D}} = \frac{2ct_{c1,2}}{\hbar} \{ & \sin\xi[\cos(\zeta x)\cos(\eta x) - \sin(\zeta x)\sin(\eta x)] \\ & - \cos\xi[\sin(\zeta x)\cos(\eta x) + \cos(\zeta x)\sin(\eta x)]\}, \end{aligned} \tag{33}$$

and is much less than the maximal velocity in the plane of the layers v_F. In Eq. (33), the following notations are used

$$\xi = \frac{cp_B}{\hbar\cos\theta}, \quad \zeta = \frac{cp_F}{\hbar}\cos\phi, \quad \eta = \frac{cp_F}{\hbar}\sin\phi, \quad x = \tan\theta. \tag{34}$$

By substituting Eq. (33) in Eq. (27) the following expression for the inter-layer electrical conductivity σ_{zz} is obtained

$$\begin{aligned} \sigma_{zz}^{\text{q1D, q2D}} = \sigma_{1,2} \Bigg\{ & J_0^2(\zeta x) J_0^2(\eta x) + \frac{2h^2}{B^2} \Bigg(J_0^2(\zeta x) \sum_{k=1}^{\infty} \frac{J_k^2(\eta x)}{\frac{h^2}{B^2} + k^2} \\ & + J_0^2(\eta x) \sum_{n=1}^{\infty} \frac{J_k^2(\zeta x)}{\frac{h^2}{B^2} + k^2} \Bigg) \Bigg\}. \end{aligned} \tag{35}$$

Here, σ_1 and σ_2 are the contributions to the conductivity in the plane of the layers from q1D and q2D carriers in the absence of a magnetic field. J_k is the k-order Bessel function and $h = \frac{m^*}{e\tau}\sqrt{1+x^2}$.

Keeping in mind the relation (32), it is not hard to show that the contribution to the σ_{yy} and σ_{zy} components of conductivity tensor from the q1D charge carriers is

$$\sigma_{yy}^{(1)} = \gamma^2\sigma_1 + \sigma_{zz}{}^{\mathrm{q1D}} \sin^2\phi \tan^2\theta \tag{36}$$

and

$$\sigma_{zy}^{(1)} = \sigma_{zz}^{\mathrm{q1D}} \sin\phi \tan\theta, \tag{37}$$

where $\gamma = 1/\omega_c\tau$.

By making use of Eqs. (24), (25) and (32), one can also find the contribution to the σ_{yy} and σ_{zy} components of conductivity tensor from the charge carriers whose states belong to the cylindrical FS

$$\sigma_{yy}^{(2)} = \gamma^2\sigma_2 + \sigma_{zz}^{\mathrm{q2D}} \tan^2\theta(\sin^2\phi - \gamma^2\cos^2\phi), \tag{38}$$

$$\sigma_{zy}^{(2)} = \sigma_{zz}^{\mathrm{q2D}} \tan\theta(\sin\phi - \gamma\cos\phi). \tag{39}$$

4. Discussion

In two-band conductors an external magnetic field affects differently the motion of charge carriers whose states belong to the weakly corrugated cylinder or corrugated plane sheets of the FS. This is why the presence of such open plane sheets of the FS is most easily revealed in a conductor placed in a magnetic field. Similarly, the contributions from different conducting channels can be detected and separated by studying thermoelectric generation of ultrasonic waves experimentally in such conductors. By far, there is no experimental evidence of this phenomenon in layered organic conductors. The present work intention is to shed light on this phenomenon in such materials and motivate new experimental research.

Below a detailed description of the evolution of Nernst effect induced ultrasonic waves ($\omega = 10^9$ Hz) with magnetic field strength, orientation and temperature presented using the parameters for the organic conductor $\alpha-(\mathrm{BEDT-TTF})_2\mathrm{KHg(SCN)}_4$. Along the z-axis the FS is slightly corrugated as a result of the finite dispersion between the layers perpendicular to the xy-plane. In the xy-plane, the FS consists of open sheets and closed cylindrical parts, from which q1D and q2D behaviors of the electronic system evolves, respectively. The results are obtained for $T = 20$ K to fields of 8 T in the normal (metallic) state of $\alpha - (\mathrm{BEDT-TTF})_2\mathrm{KHg(SCN)}_4$ and the strength of the two conducting channels is taken to be $\sigma_1/\sigma_2 = 2$.[14]

4.1. *Boundary conditions and wave generation*

Figure 1 shows the amplitude of the generated due to Nernst effect wave as a function of a magnetic field for both isothermal and adiabatic boundary at $T = 20$ K and

several field directions from the normal to the layers: $\theta = 3°, 16°, 28°, 47°, 60°$ and $85°$. The in-plane angle is fixed to $89°$ so that the field rotation is in the yz-plane.

It can be seen from Fig. 1 that the $U_{zl}(B)$ curves do not increase with increasing angle θ between the normal to the layers and magnetic field but rather show a periodic dependence of the amplitude on the tilt angle. This is correlated with the magnetic field and angular behavior of Nernst effect N_{zy} (Fig. 4) as discussed below.

Magnetic field dependences reveal distinct boundary preferences for the longitudinal wave generation. In the case of an isothermal boundary (solid curves in Fig. 1), the wave generation starts at zero magnetic field, reaches a clearly marked maximum at $B \sim 2.6$ T for all field directions θ from the normal to the layers and then decreases monotonically. Below the maximum value, the amplitude assumes linear in field dependence, $U_{zl}(B) \sim B$ while above it decreases in proportion to B^{-1}. For an adiabatic boundary (dashed curves), the generation is largest at $B = 0$ for all θ due to the nonzero temperature distribution at $z = 0$. With increasing field, the amplitude is decreasing as B^{-1} in the whole range of magnetic fields. Most strikingly, at $B > 4$ T, the amplitude for the adiabatic boundary is smaller than the amplitude for the isothermal boundary for all field directions despite the existence of a heat flux through the conductor's surface in the latter case. Thus, by comparing the influence of boundary conditions, both mechanical and thermal, the efficiency of the linear thermoelectric ultrasonic wave generation can be estimated. This would be useful when performing experiments for explaining the magnitude of experimentally measured efficiency or amplitude of the generated wave in the case of different boundaries. If the boundary is mechanically free (as considered here), the case of an adiabatic boundary is preferable at low fields (below $B = 4$ T) while

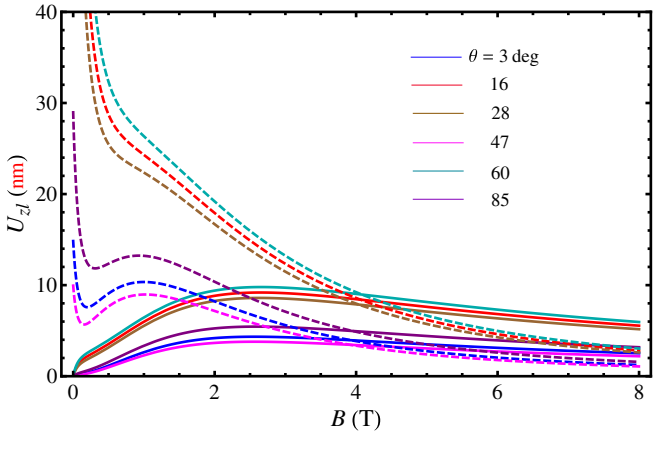

Fig. 1. (Color online) The magnetic field dependence of the longitudinal ultrasonic wave amplitude $U_{zl}(B)$ excited by the Nernst effect for isothermal (solid curves) and adiabatic boundary (dashed curves) at $T = 20$ K, $\phi = 89°$ and several field directions from the normal to the layers: $\theta = 3°, 16°, 28°, 47°, 60°$ and $85°$. The curves for $\theta = 16°, 28°$ and $60°$ obtained for adiabatic boundary are scaled for clarity.

isothermal boundary is preferable for fields $B > 4$ T. This behavior is completely different in comparison to the conductors with only q2D charge carriers[12] where the acoustic wave is attenuated at low fields ($B \sim 0.6$ T) and the adiabatic amplitude exceeds the isothermal in the whole range of B.

4.2. *Temperature dependent wave amplitude*

The preference of one type of boundary over another is as well reflected in the temperature dependence of the wave amplitude $U_{zl}(T)$ as both the field and angle are changed (Fig. 2). The wave amplitude and thermal skin depth are temperature dependent as $U_{zl}(T) \sim T^2$ and $\delta_T(T) \sim T^{1/2}$ (inset in Fig. 2).

Below $T = 20$ K, $U_{zl}(T)$ is negligibly small and close in value for each B and θ (for $T \leq 10$ K the amplitude is the same for each B and θ) and $\delta_T(T)$ tends to collapse into one curve. This could suggest an existence of a specific behavior of the organic conductors at low temperatures ($T \leq 10$). For example, organic conductors of the family $\alpha - (\mathrm{BEDT} - \mathrm{TTF})_2\mathrm{MHg(SCN)}_4$ exhibit a phase transition from normal to a charge density wave state at $T \leq 10$ ($T = 8$ K for M = K[15] and 10 K for M = Tl,[16] Rb[17]).

At $B \sim 4$ T both amplitudes are equal as shown in Fig. 2 for $B = 4.05$ T, $\theta = 16°$ (blue curve) and $B = 3.93$ T, $\theta = 47°$ (magenta curve). Below (above) this field the adiabatic amplitude $U_{zl}(T)$ is always larger (smaller) than the isothermal.

At lower temperatures, when $|k_T| \ll |k|$ or $\delta_T \gg \delta_E$, the temperature distribution at large distance from the conductor's surface is determined by the thermal, and not electrodynamic characteristics of the conductor. The thermal field attenuates at distance δ_T within the conductor and, when $\delta_T \gg \delta_E$, the coupling between

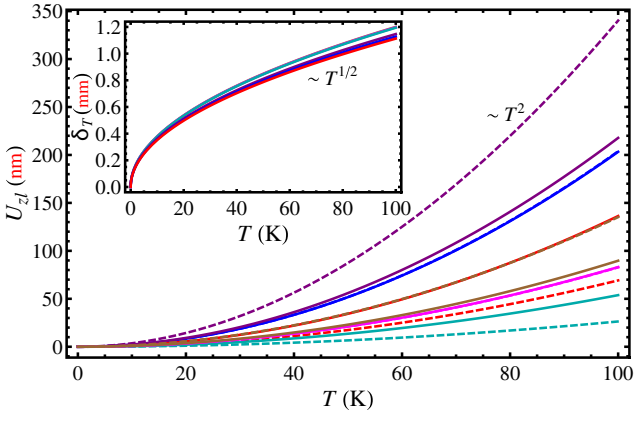

Fig. 2. (Color online) The temperature dependence of the amplitude of the ultrasonic wave $U_{zl}(T)$ for isothermal (solid curves) and adiabatic boundary (dashed curves) at $\phi = 89°$ and the following set of fields B and angles θ: $B = 2.6$ T, $\theta = 16°$ (purple); $B = 4.05$ T, $\theta = 16°$ (blue); $B = 8$ T, $\theta = 16°$ (red); $B = 2.6$ T, $\theta = 47°$ (brown); $B = 3.93$ T, $\theta = 47°$ (magenta); $B = 8$ T, $\theta = 47°$ (cyan). The inset shows the temperature dependence of the thermal skin depth $\delta_T(T)$ for the same set of fields and angles. The colors of the curves are the same as in the main panel.

the electromagnetic and thermal oscillations is weak which in turn decreases the wave amplitude. In the case of an adiabatic boundary, due to the fixed boundary condition, a large part of the heat source energy remains in the electromagnetic wave and dissipates at distance $\sim \delta_E$. Therefore, the wave amplitude for the adiabatic boundary, $U^a_{zl} \simeq \frac{1}{q\delta_E} U^i_{zl}$, decreases faster than the amplitude for the isothermal boundary above certain field.

4.3. *Electromagnetic and thermal skin depth in two-band organic conductors*

In presence of an additional group of charge carriers with a q1D energy spectrum, high-frequency properties of the layered organic conductors are quite sensitive not only to the polarization of the incident wave but also to the direction of propagation of electromagnetic field in the plane of the layers. Both the electromagnetic δ_E and thermal δ_T skin depth are plotted as a function of the magnetic field in Fig. 3.

The electromagnetic skin depth $\delta_E \sim \frac{B}{h}(\frac{2}{\omega\mu_0(\sigma_1+\sigma_2)})^{1/2}$ increases as magnetic field increases with proportion to B^1. The thermal skin depth $\delta_T \sim 2\frac{h}{B}(\frac{\sigma_1+\sigma_2}{\omega C})^{1/2}$ decreases with field approximately proportional to B^{-1}. This corroborates the above observed behavior of the ultrasonic wave amplitude with increasing field. For isothermal boundary, due to the zero temperature distribution $(\Theta|_{z=0} = 0)$ at the surface, at low fields the wave is transmitted by the electromagnetic field propagating along the y-axis and $U_{zl}(B)$ increases with field as $\delta_E(B) \sim B^1$. With increasing field, as the temperature distribution for $z > 0$ increases, the $U_{zl}(B)$ dependence is determined by the thermal field along the z-axis and decreases as $\delta_T(B) \sim B^{-1}$. For adiabatic boundary, due to nonzero temperature distribution at the surface, the wave is transmitted by the thermal field in a wide range of magnetic fields and $U_{zl}(B)$ decreases with increasing field as $\delta_T(B) \sim B^{-1}$. In

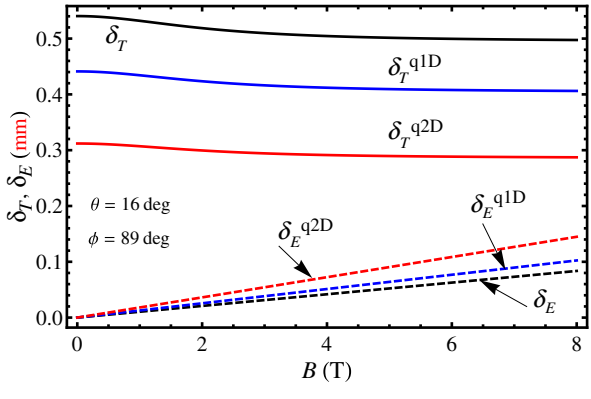

Fig. 3. (Color online) Magnetic field dependence of the electromagnetic $\delta_E(B)$ and thermal $\delta_T(B)$ skin depths for $T = 20$ K, $\theta = 16°$ and $\phi = 89°$. Black curves represent the total electromagnetic and thermal depth. Blue and red curves represent the contributions to $\delta_E(B)$ and $\delta_T(B)$ from the q1D and q2D charge carriers, respectively. The curves for $\delta_E(B)$ are scaled by factor 3 for clarity.

$\alpha - (\mathrm{BEDT-TTF})_2\mathrm{KHg(SCN)}_4$, δ_E is linear in field (dashed curves in Fig. 3) in agreement with the experiment[18] while δ_T decreases slightly with increasing field to $B = 4$ T above which is weakly field dependent. This coincides with a field at which both amplitudes are the same as evident from the magnetic field and temperature dependence of U_{zl}. Above $B = 4$ T, the small change in δ_T indicates that the acoustic wave is not strongly attenuated with increasing field as observed from $U_{zl}(B)$ curves in Fig. 1. In addition, the calculated contributions to δ_E and δ_T from the two conducting channels show that when $\sigma_1 > \sigma_2$ then $\delta_E^{\mathrm{q1D}} < \delta_E^{\mathrm{q2D}}$ and $\delta_T^{\mathrm{q1D}} > \delta_T^{\mathrm{q2D}}$. It follows that the presence of a group of charge carriers with q1D energy spectrum does not affect significantly the attenuation length of an electromagnetic wave that propagates along the y-axis but does affect the attenuation length of the thermal field along the z-axis in the conductor.

4.4. *The role of Nernst effect in wave generation*

The ultrasonic waves are generated due to the Nernst effect N_{zy} and therefore, it is instructive to discuss the results for the amplitude through how Nernst effect changes with field and angle (Fig. 4).

For the given magnetic field in-plane direction, $\phi = 89°$, $N_{zy}(B)$ curves calculated for the same field directions θ as in Fig. 1 are close to each other which means that in the metallic state the Nernst effect does not change much with the angle θ. However, we found that there is a grouping of the $N_{zy}(B)$ curves with the angle θ which is also observed in the $U_{zl}(B)$ dependence (Fig. 1). The reason for this behavior is the periodic oscillations of the Nernst effect when a constant magnetic field is turned from the direction normal to conducting layers toward the plane of the layers.[19–21] In layered organic conductors, numerous drastic deviations from the conventional three-dimensional behavior and even qualitatively new effects, in

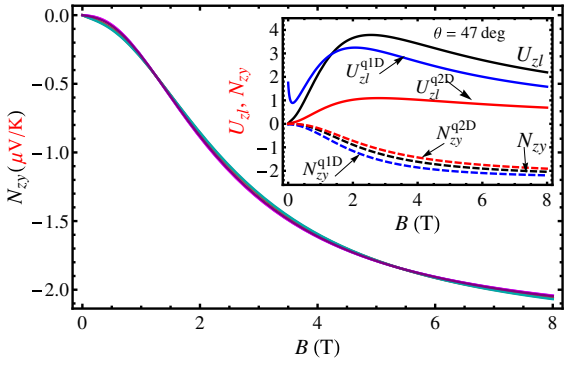

Fig. 4. (Color online) The magnetic field dependence of the Nernst effect N_{zy} at $T = 20$ K, $\phi = 89°$ and the same field directions θ as in Fig. 1. The inset shows the ultrasonic wave amplitude U_{zl} for isothermal boundary condition (solid black curve) and Nernst effect N_{zy} (dashed black curve) at $\theta = 47°$ and the corresponding contributions from the q1D (blue curves) and q2D charge carriers (red curves).

particular related to the field orientation, have been found. Among them are the angular oscillations of the kinetic and thermoelectric coefficients associated with the periodic dependence of the average electron velocity along the z-axis, $\bar{v}_z$, on the tilt angle θ. Since the ultrasonic waves are generated due to thermoelectric effect, it is also expected the angular oscillations of the wave amplitude to emerge when tilting the field from the normal to the layers. Hence for some angles, the Nernst effect could be zero, but for other angles, it has maximum or minimum depending on the value of the average electron velocity $\bar{v}_z$. This implies that the interaction of charge carriers with the wave will be effectively different for different angles θ and the $U_{zl}(B)$ curves (Fig. 1) would exhibit periodic dependence with increasing angle.

Here, $N_{zy}(B)$ is negative, i.e., electron-like for each field direction from the normal to the layers implying that the contribution of the q1D electron-like carriers in both the Nernst effect and wave amplitude is significant. In that respect, the inset in Fig. 4 shows the corresponding contributions to $U_{zl}(B)$ and $N_{zy}(B)$ from the two conducting channels. As expected, the presence of q1D charge carriers changes the entire picture of the propagation of ultrasonic wave in a magnetic field tilted away from the plane of the layers. Moreover, in the case of isothermal boundary, $U_{zl}(B)$ does not reach a maximum at the same magnetic field for the two conducting channels. This is correlated with a change of the slope of δ_T^{q1D} and δ_T^{q2D} which occurs at different magnetic field for both thermal skin depths. The field at which the change of the slope in thermal skin depths occurs can be identified by a maximum in $U_{zl}^{\mathrm{q1D}}(B)$ and $U_{zl}^{\mathrm{q2D}}(B)$, respectively. The total wave amplitude $U_{zl}(B)$ reaches a maximum at the mid-field ($B \sim 2.6$ T) between the two maxima of $U_{zl}^{\mathrm{q1D}}(B)$ and $U_{zl}^{\mathrm{q2D}}(B)$, as seen from the inset in Fig. 4. However, an experimental research is necessary in order to reveal if this behavior is a common feature of two-band organic conductors due to the coexistence of a q2D cylinder and q1D sheets.

4.5. *Possibilities for experimental studies of linear thermoelectric wave generation in two-band organic conductors*

The observation of thermoelectric generation of ultrasonic waves is constraint by the condition $\omega\tau \ll 1$. In two-band organic conductors $\alpha-(\mathrm{BEDT-TTF})_2\mathrm{MHg(SCN)}_4$ this condition is always fulfilled as the relaxation time τ is very small (for $\alpha-(\mathrm{BEDT-TTF})_2\mathrm{KHg(SCN)}_4$, $\tau = 2\times10^{-12}$ s[22]). In addition, for the generation of ultrasonic waves to be most effective, other conditions must be satisfied. This includes fulfillment of $q\delta_E, q\delta_T \ll 1$ as long as the conditions for normal skin effect $kl, k_T l \ll 1$ are satisfied. In the present case, for $\alpha-(\mathrm{BEDT-TTF})_2\mathrm{KHg(SCN)}_4$, following values are obtained: $\delta_E = 25$ μm and $\delta_T \sim 0.5$ mm at $B = 8$ T. Since the Fermi velocity is of order $v_F = 6.5\times10^4$ m/s[23] the electron mean free-path is $l = v_F\tau = 130$ nm. It is evident that the necessary conditions are fulfilled even at higher fields providing the ultrasonic wave generation to be studied in detail experimentally in a wide range of magnetic fields.

Experiments on thermoelectric generation of ultrasonic waves in layered organic conductors would be favorable for a number of reasons. First, these compounds are highly pure that makes them very convenient for performing experiments. Second, samples are usually small in size (several millimeters) and fragile. Therefore, using couplants can be very cumbersome to deal with especially when performing experimental measurements on thermoelectric coefficients in the presence of a temperature gradient. In thermoelectric measurements, there is always the possibility of random diffusion of heat along the sample due to a misalignment between the heat current and the crystal axes. Also, the total thermopower and Nernst effect may involve a mixing of contributions from several bands since in a two-band system there is a mixing between the states on the two FS sections. Using noncontact ultrasonic techniques involving thermoelectric generation of ultrasonic waves would make it possible to obtain the magnetic field and angular dependences of Nernst effect especially in complex systems as $\kappa - (\mathrm{BEDT-TTF})_2\mathrm{Cu(SCN)}_2$ and $\alpha - (\mathrm{BEDT-TTF})_2\mathrm{MHg(SCN)}_4$ from the field and angular dependences of detected ultrasound. Third, ultrasonic measurements are known to be a powerful tool for studying magnetic phase transitions in materials. This can be used to study the complex ground state in $\alpha - (\mathrm{BEDT-TTF})_2\mathrm{KHg(SCN)}_4$ which develops at lower temperatures due to a phase transition from a metallic to an insulating density wave state. The true nature of the low temperature ground state of this conductor is still a subject of contemporary debate. Fourth, ultrasonic measurements can be used to study the gap in the electronic structure as well as the inter- and in-plane electronic anisotropy in these materials arising from their complex structure. Fifth, by studying the changes in field and angular dependences of the attenuation and efficiency of the linear thermoelectric ultrasonic wave generation one can obtain the contributions from different groups of charge carriers in the effect for different geometries, i.e., different polarization and direction of propagation of the wave. For example, in $\alpha - (\mathrm{BEDT-TTF})_2\mathrm{KHg(SCN)}_4$ the x-axis is the most and the z-axis is the least conducting directions so that it is expected that the amplitude of the generated wave and thus the efficiency of the effect would be completely different for both directions. In the former it is expected the q1D conducting channel to dominate by far the effect that would lead to distinct acoustic properties compared to those observed in the latter.

5. Conclusions

The linear thermoelectric generation of ultrasonic waves ($\omega = 10^9$ Hz) in layered organic conductors with two groups of charge carriers (q1D and q2D) is considered. The amplitude of the generated wave due to Nernst effect is analyzed as a function of the magnetic field B, the temperature T, the angle between the normal to the layers and the magnetic field θ as well as of the characteristics of the conductor: electromagnetic δ_E and thermal δ_T skin depth, Nernst effect N_{zy} and inverse thermal conductivity κ_{zz}^{-1}. Specifically, the parameters for the two-band organic conductor

$\alpha-(\mathrm{BEDT-TTF})_2\mathrm{KHg(SCN)}_4$ are used to obtain the wave amplitude in its normal (metallic) state. It has been shown that the necessary conditions for observing the linear thermoelectric generation are fulfilled even in relatively high but nonquantizing magnetic fields to 8 T. In addition, the changes in the amplitude are studied through how Nernst effect changes with the magnetic field strength. The magnetic field dependence reveals different behavior of the wave amplitude depending on the boundary conditions. For isothermal boundary, the amplitude is increasing linearly in field up to $B \sim 2.6$ T and then decreases approximately as B^{-1} for each field direction. For adiabatic boundary, the amplitude is decreasing following the B^{-1} dependence. This behavior is correlated with the boundary conditions at the surface and the corresponding field dependence of the electromagnetic $\delta_E(B)$ and thermal skin depth $\delta_T(B)$.

An important feature to emphasize is that at $B = 4$ T both amplitudes are equal in value but above this field the amplitude for the adiabatic boundary becomes smaller than the one for the isothermal boundary although there is a presence of a heat flux in the latter. This defines the preference of one type of a boundary over another which is significant when performing experimental measurements. The temperature dependence confirms this unusual behavior of the generated ultrasonic wave. For the adiabatic case, the acoustic wave is dragged by the thermal field in a wide range of magnetic fields but due to the fixed boundary condition, a part of the heat source energy is "captured" by the electromagnetic field which dissipates at distance of order of the electromagnetic skin depth δ_E. In comparison, for the isothermal case, due to the nonfixed boundary condition, the acoustic wave is transmitted by the thermal wave which dissipates at distance of order of the thermal skin depth δ_T.

The calculated contributions from the two groups of charge carriers to the wave amplitude, Nernst effect as well as the skin depths show that both carriers are involved in the thermoelectric generation of ultrasonic waves and the presence of a group of charge carriers with q1D energy spectrum affects significantly the attenuation of both the thermal field and ultrasonic wave along the z-axis. Another important feature to emphasize is that, for the isothermal case, the magnetic field at which the amplitude is maximum differs for the two groups of carriers. As a result, the total amplitude reaches a maximum at the mid-field between these two maxima. This is associated with the complex Fermi surface in two-band organic conductors.

In two-band organic conductors, the conditions for thermoelectric generation of ultrasonic waves are fulfilled for a wide range of magnetic fields. This could allow to investigate existing problems in these materials through experimental studies that involve linear wave generation using noncontact ultrasonic techniques.

References

1. H. Mori *et al.*, *Bull. Chem. Soc. Japan* **63**, 2183 (1990).

2. R. Rousseau *et al.*, *J. Phys. 1* **6**, 1527 (1996).
3. V. M. Kontorovich, *Sov. Phys. JETP* **18**, 1125 (1964).
4. V. M. Kontorovich, *Sov. Phys. JETP* **32**, 1146 (1971).
5. M. I. Kaganov and V. M. Cukernik, *Zh. Eksp. Teor. Fiz.* **35**, 474 (1958).
6. M. I. Kaganov, *Zh. Eksp. Teor. Fiz.* **98**, 1828 (1990).
7. M. I. Kaganov and F. M. Maallavi, *Fiz. Nizk. Temp.* **18**, 737 (1992).
8. A. N. Vasil'ev, F. M. Maallavi and M. I. Kaganov, *Phys. Usp.* **36**, 968 (1993).
9. A. V. Andrianov *et al.*, *JETP* **94**, 277 (1988).
10. I. E. Aronov and V. L. Fal'ko, *Phys. Rep.* **221**, 81 (1992).
11. M. I. Kaganov and A. N. Vasil'ev, *Die Kunst of Phonons-Lectures from the Winter School of Theoretical Physics*, eds. T. Paszkiewicz *et al.*(Springer, 1994), pp. 399–405.
12. D. Krstovska, O. Galbova and T. Sandev, *Europhys. Lett.* **81**, 37006 (2008).
13. A. A. Abrikosov, *Fundamentals of the Theory of Metals* (North-Holland, Amsterdam, 1988).
14. B. Dóra *et al.*, *Europhys. Lett.* **60**, 737 (2002).
15. T. Sasaki *et al.*, *Solid State Commun.* **75**, 39 (1990).
16. N. Kinoshita, M. Tokumoto and N. Anzai, *J. Phys. Soc. Jpn.* **60**, 2131 (1991).
17. N. D. Kusch *et al.*, *Synth. Met.* **46**, 271 (1992).
18. N. Harrison *et al.*, *J. Phys.: Condens. Matter* **13**, L389 (2001).
19. E. S. Choi, J. S. Brooks and J. S. Qualls, *Phys. Rev. B* **65**, 205119 (2002).
20. D. Krstovska *et al.*, *Low Temp. Phys.* **37**, 950 (2011).
21. D. Krstovska *et al.*, *J. Phys.: Condens. Matter* **24**, 265502 (2012).
22. N. Harrison *et al.*, *Phys. Rev. B* **54**, 9977 (1996).
23. A. E. Kovalev, S. Hill and J. S. Qualls, *Phys. Rev. B* **66**, 134513 (2002).